JOURNAL OF MATERIALS SCIENCE 12 (1977) 1115–1124

The thermal decomposition of ammonium paratungstate

A. K. BASU, F. R. SALE
Metallurgy Department, Manchester University, Joint University and UMIST Metallurgy Building, Grosvenor Street, Manchester, UK

The thermal decomposition of monoclinic, orthorhombic and freeze-dried ammonium paratungstate (APT) has been studied over the temperature range 100 to 500° C using thermogravimetry, evolved gas analysis, X-ray diffraction and electron optical techniques. The particle morphologies of the original APT have been related to the morphologies of the products of decomposition. A mechanism of decomposition which postulates the formation and subsequent decomposition of amorphous ammonium metatungstate is proposed and substantiated by X-ray diffraction analysis and evolved gas analysis.

1. Introduction

The thermal decomposition of solid ammonium paratungstate (APT) to tungsten oxide, prior to hydrogen reduction, is an essential first step in the production of tungsten powder. The particle size and morphology of the tungsten powder are greatly influenced by the particle size and morphology of the oxide material which, in turn, depend on the characteristics of the APT.

A number of techniques [1–6] have been applied from time to time for the production of tungsten powder with a view to obtaining superior properties in the ultimate products. However, time has shown the potential advantages of the hydrogen reduction APT route over other successful but less commonly used methods, especially the chloride reduction method which is useful for the production of submicron metal powder. Furthermore, most of the capital investment at the present time is associated with the APT process. The demand for submicron tungsten powder is also comparatively small and in the majority of circumstances does not warrant additional huge investment on an entirely new process at the present time. Consequently, there exists considerable interest in ways of modifying the APT process such that submicron powders may be produced.

The freeze-drying of inorganic solutions has been reported as a possible process for the production of fine powders and homogeneous powder mixtures in recent years [7–9]. Consequently, investigations have been carried out on the decomposition of conventionally crystallized and freeze-dried samples of APT to determine the effect of the APT morphology on the kinetics of decomposition and morphologies of the resultant oxide products. The present paper also proposes a mechanism of decomposition of APT which is substantiated by X-ray diffraction studies of the products of partial decomposition and by evolved gas analysis.

2. Experimental procedure and results

2.1. Materials

The methods used for the preparation of five commercial samples of APT and the characterization of these samples have been described elsewhere [10]. From the initial characterization of these samples, three representative samples were chosen for further study. Three of the original samples had an identical crystal structure and very similar particle morphologies. It was, therefore, anticipated that these would behave in a similar manner under identical experimental conditions. Consequently, the samples chosen for further comparison are shown in Figs. 1 to 3, and are the monoclinic pentahydrate APT, the orthorhombic undecahydrate APT and the freeze-dried sample of APT, which have different particle morphologies.

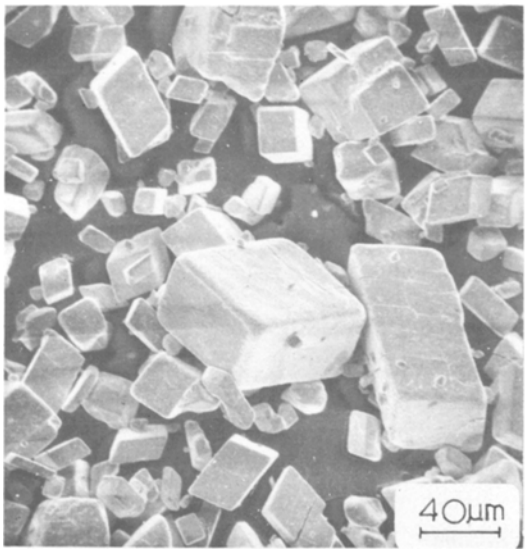

Figure 1 Monoclinic pentahydrate APT.

Figure 2 Orthorhombic undecahydrate APT.

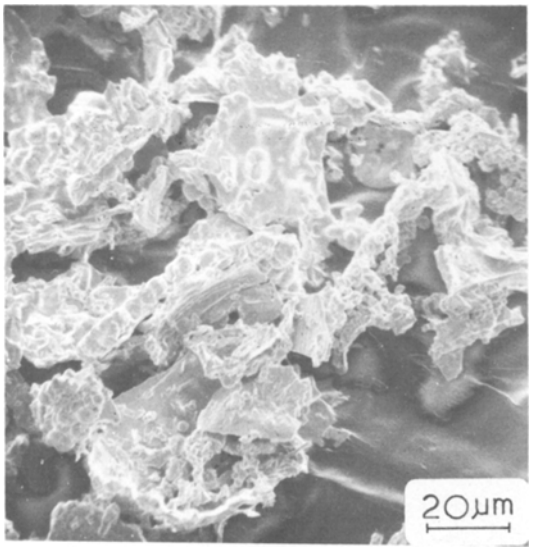

Figure 3 Freeze-dried APT.

2.2. Thermal decomposition

A simple glass-spring thermogravimetric balance was used in conjunction with a furnace for the study, because it could be used to follow the kinetics of decomposition of a sample, and allow easy retrieval of the product for subsequent characterization by X-ray diffraction and scanning electron-optical techniques. The apparatus is shown schematically in Fig. 4.

The thermal decomposition of APT was carried out in a nitrogen atmosphere. Gas from a cylinder passed past a relief tube filled with di-*n*-butyl phthalate and then through a flowmeter and a drying tower filled with anhydrous calcium chloride before being admitted to the furnace.

In operation, approximately 0.5 g of an APT sample was accurately weighed in a nickel pan and suspended in the hot zone of the furnace. Dry nitrogen was flushed through the apparatus for about 1 h at room temperature to remove the residual air from inside the system. The temperature of the furnace was subsequently increased at 10° C min^{-1} in 100° C intervals. At each temperature of 100, 200, 300 and 400° C the sample

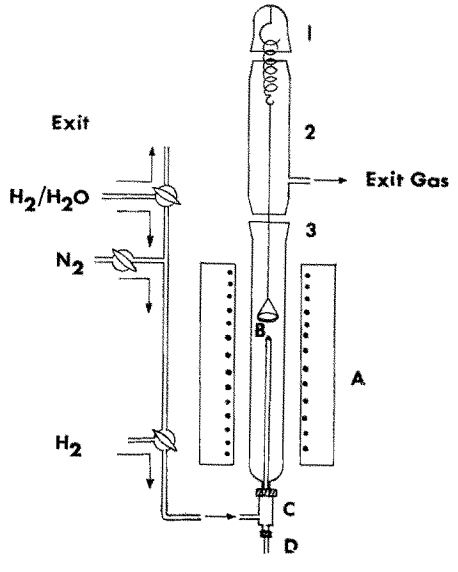

Figure 4 Glass-spring thermobalance.

TABLE I Evolved gas analysis during decomposition of ammonium paratungstate

Sample	Mass number	Peak heights (arbitrary units)					
		Background	100° C	200° C	300° C	400° C	500° C
Orthorhombic APT	14	–	–	0.16	0.16	0.06	–
	15	–	–	0.80	0.90	0.70	0.45
	16	0.11	0.30	18.40	17.36	13.86	9.32
	17	0.04	0.18	22.43	21.60	17.13	11.11
	18	3.30	5.30	9.00	12.60	12.50	11.70
	28	1.25	1.40	2.00	2.00	2.00	3.00
Monoclinic APT	14	–	–	0.15	–	0.06	–
	15	–	–	0.60	0.40	0.50	0.18
	16	0.16	0.14	12.66	16.38	11.38	2.80
	17	–	–	15.55	36.52	13.47	2.84
	18	3.60	5.75	8.04	10.80	11.00	10.08
	28	2.60	1.30	2.10	5.00	2.00	1.80
Freeze-dried APT	14	–	–	0.05	0.05	0.07	0.04
	15	–	–	0.30	0.60	0.39	0.30
	16	0.12	0.79	9.33	16.87	11.92	10.42
	17	0.03	0.66	20.35	22.88	14.84	14.18
	18	2.50	5.85	6.75	7.50	7.20	7.50
	28	1.60	1.30	1.40	1.80	1.50	1.55

was held for 2 h until no further weight loss was detected. After decomposition the sample was cooled to room temperature in the furnace in the nitrogen atmosphere. Fig. 5 gives the relationship between the % decomposition and temperature for the three samples of APT.

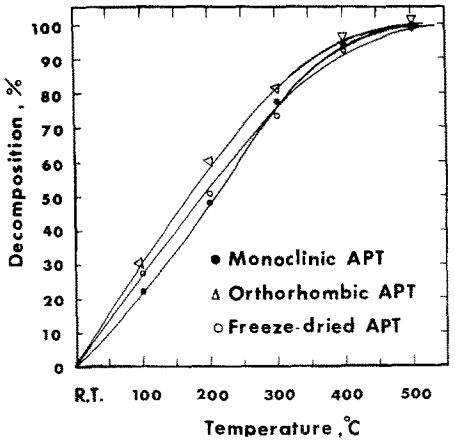

Figure 5 Relationship between % decomposition and temperature for the APT samples.

2.3. Evolved gas analysis

Evolved gas analysis was carried out using a "VG Micromass 6" mass spectrometer. The resolving slit used was 0.05 mm which gave a resolution of approximately 400 at mass 40.

The system used for this study had an internal volume of approximately 15 ml and consisted of a small diameter (8 mm) vertical tube with a bulb at the bottom to retain a known weight of the sample. The tube was attached by means of a cup and cone arrangement to a high vacuum tap to facilitate evacuation of the system by a rotary pump. A capillary tube and glass sinter comprised the inlet to the source of the mass spectrometer.

The tube containing a known weight of the sample (approximately 0.14 g) in the bulb was inserted into the hot zone of a furnace. The mass spectrometer was operated to scan continuously over the mass range 1 to 40. The sample was heated in stages of 100° C to a temperature of up to 500° C and the evolved gases were continuously analysed. Table I shows the results of the evolved gas analysis.

TABLE II *d* spacings and the intensities of the major lines obtained for the samples of APT after full decomposition

d spacings (Å)	I/I_1	Phase	*d* spacings (Å)	I/I_1	Phase
3.85	100	WO_3	1.89	16	WO_3
3.74	90	$WO_{2.9}$	1.82	20	WO_3
3.69	85	WO_3	1.81	25	WO_3
3.35	10	WO_3	1.71	10	WO_3
3.10	30	WO_3	1.67	10	WO_3
2.65	60	$WO_{2.9}$	1.66	10	WO_3
2.63	63	WO_3	1.64	15	WO_3
2.52	10	WO_3	1.53	7	$WO_{2.9}$
2.17	25	WO_3	1.49	10	WO_3
1.92	16	WO_3	1.25	20	$WO_{2.9}$

TABLE III *d* spacings and intensities of the major lines obtained for the incomplete decomposition of monoclinic APT

Decomposed at 315° C			Decomposed at 350° C					
d spacing (Å)	I/I_1	Phase	*d* spacing (Å)	I/I_1	Phase	*d* spacing (Å)	I/I_1	Phase
8.56	100	Monoclinic APT	6.48	16	Monoclinic APT	1.87	4	WO_3
6.48	20	Monoclinic APT	3.85	86	WO_3	1.83	14	Orthorhombic APT
3.85	10	WO_3	3.75	78	WO_3	1.82	14	WO_3
3.75	10	WO_3	3.69	100	WO_3	1.80	16	WO_3
3.47	30	Orthorhombic APT	3.35	7	WO_3	1.71	8	WO_3
3.11	40	Orthorhombic APT	3.16	25	Orthorhombic APT	1.64	18	WO_3
2.98	40	Orthorhombic APT	3.10	25	WO_3	1.49	6	WO_3
2.89	50	Monoclinic APT	2.76	7	Monoclinic APT			
			2.68	50	WO_3			
			2.63	57	WO_3			
			2.44	15	Orthorhombic APT			
			2.17	20	WO_3			
			1.99	10	WO_3			
			1.92	12	WO_3			

TABLE IV *d* spacings and intensities of the major lines obtained for the incomplete decomposition of orthormbic APT

Decomposed at 315° C			Decomposed at 350° C					
d spacing (Å)	I/I_1	Phase	*d* spacing (Å)	I/I_1	Phase	*d* spacing (Å)	I/I_1	Phase
3.85	100	WO_3	6.48	16	Monoclinic APT	2.63	35	WO_3
3.75	80	WO_3	3.85	100	WO_3	2.44	25	Orthorhombic APT
3.69	95	WO_3	3.75	80	WO_3	2.17	10	WO_3
3.16	72	Orthorhombic APT	3.69	95	WO_3	1.92	5	WO_3
2.65	50	Orthorhombic APT	3.35	10	WO_3	1.87	3	WO_3
2.45	60	Orthorhombic APT	3.28	10	Monoclinic APT	1.83	30	WO_3
1.83	48	Orthorhombic APT	3.16	50	Orthorhombic APT	1.80	10	WO_3
1.66	40	WO_3	3.10	15	WO_3	1.71	10	WO_3
1.59	20	WO_3				1.64	20	WO_3
						1.59	7	WO_3

TABLE V *d* spacings and intensities of the major lines obtained for the incomplete decomposition of freeze-dried APT

Decomposed at 315° C			Decomposed at 350° C					
d spacing (Å)	I/I_1	Phase	*d* spacing (Å)	I/I_1	Phase	*d* spacing (Å)	I/I_1	Phase
6.48	30	Monoclinic APT	6.48	16	Monoclinic APT	2.44	25	Orthorhombic APT
3.85	40	WO_3	3.85	100	WO_3	2.17	10	WO_3
3.16	100	Orthorhombic APT	3.75	80	WO_3	1.92	5	WO_3
2.92	16	Orthorhombic APT	3.69	95	WO_3	1.87	3	WO_3
2.65	16	Orthorhombic APT	3.35	10	WO_3	1.83	30	WO_3
2.45	64	Orthorhombic APT	3.28	10	Monoclinic APT	1.80	10	WO_3
1.83	25	Orthorhombic APT	3.16	50	Orthorhombic APT	1.71	10	WO_3
1.64	23	WO_3	3.10	15	WO_3	1.64	20	WO_3
			2.68	25	Monoclinic APT	1.59	7	WO_3
			2.63	35	WO_3			

2.4. X-ray diffraction analysis

The fully decomposed samples were analysed in a "Siemens Kristalloflex" diffractometer using Cu$K\alpha$ radiation. All the samples of APT after complete decomposition gave identical *d* spacings and intensities, which together with the identified phases are listed in Table II.

The samples of APT were also decomposed at temperatures corresponding to 25, 50 and 75% decompositions and higher. The products were cooled under nitrogen in the furnace and were later analysed by X-ray diffraction in order to determine the sequence of decomposition of APT to the tungsten oxide. The results are shown in Tables III to V for the three types of APT.

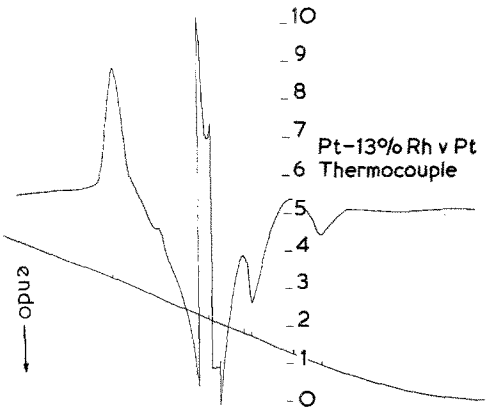

Figure 6 DTA curve for monoclinic APT.

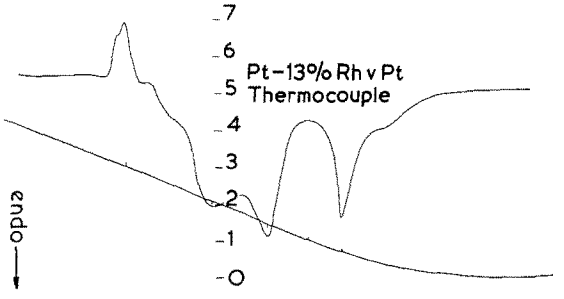

Figure 7 DTA curve for orthorhombic APT.

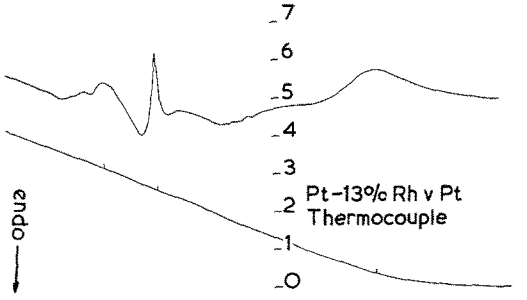

Figure 8 DTA curve for freeze-dried APT.

2.5. Differential thermal analysis

The decomposition of the samples of APT was studied in a "Stanton" Differential Thermal Analysis Equipment "Standata" model 6–25. The sample was heated in an inconel crucible (8 mm diameter and 10 mm depth) from room temperature to 500° C at a rate of 5° C min^{-1} in a nitrogen atmosphere using alumina as the reference material. Figs. 6 to 8 show the nature of the enthalpy change against temperature for the samples studied.

TABLE VI Particle size analysis of monoclinic APT after thermal decomposition

Temperature of decomposition (° C)	Average diameter (μm)	Number of particles	Total volume (μm^3)	Weight %
500	5.1	2653	186 443	0.6
	12.9	1708	1 901 995	6.1
	21.4	929	4 793 909	15.4
	30.4	527	7 465 213	24.0
	38.6	313	9 410 890	30.2
	47.2	134	7 359 119	23.6
800	5.1	1232	86 580	3.2
	12.9	1209	1 346 322	5.0
	21.4	713	3 679 286	13.7
	30.3	427	6 048 666	22.5
	38.6	279	8 388 620	31.2
	47.2	133	7 304 200	27.2

2.6. Particle size and morphology

The morphologies of the products of thermal decomposition of the three samples of APT were observed in a "Cambridge Stereoscan 180" scanning electron microscope. The samples were prepared in the same manner as described earlier [10].

The accelerating voltage used was of the order of 25 to 30 kV. Figs. 9 to 11 show the overall particle morphologies of the samples. The measurement of particle size distribution was attempted with a "Metals Research Quantimet Image Analysing Computer – Quantimet 720". Two methods were used to obtain the experimental data from the instrument. In some cases, samples were prepared by carefully sprinkling the powder on a glass slide so that each particle on the slide was distinctly separated from the other. In other cases, particle size distribution was obtained from the processing of the electron micrographs of the samples when the Quantimet was operated in conjunction with an epidiascope. Table VI gives the results of the particle size distribution in the products of decomposition of the monoclinic sample of APT at 500 and 800° C. The measurements were also carried out on the other samples, but since they were found to be very difficult to separate into individual particles during sample preparation, the results obtained for them were ignored.

3. Discussion

3.1. Kinetics of decomposition

It can be seen from Fig. 5 that all the samples of APT were fully decomposed at temperatures above 450° C. It was found that increase in the holding

time beyond an initial period of 10 to 15 min at temperatures below 450° C did not increase the % decomposition of the sample beyond the value for that particular temperature given in Fig. 5. Since the samples of orthorhombic undecahydrate APT and the freeze-dried APT correspond to the composition $5(NH_4)_2.O.12WO_3.11H_2O$, the greater rate of weight loss for these samples observed in the initial part of decomposition (up to 300° C), compared to the monoclinic APT which had the composition $5(NH_4)_2O.12WO_3.5H_2O$, was caused by the greater loss of combined water. Apart from these slight differences in the initial stages, the kinetics of decomposition of the different samples can be seen to be similar and the difference in the particle morphologies of the samples has negligible effect on the kinetics of decomposition.

3.2. Evolved gas analysis

It was found that on heating from room temperature to 100° C, the decomposition of all the samples was initiated by the evolution of water vapour, as was evident from the increase in corrected peak heights at mass number 18; however, very small amounts of ammonia were evolved at this stage (Table I). This water vapour evolution corresponds to the endothermic peaks in the initial part of the thermograms obtained by DTA given in Figs. 6 to 8. Further increases in temperature caused the evolution of a large quantity of ammonia as observed from the dramatic increase in peak heights at mass numbers 15, 16 and 17 at 200° C compared to that of the background at room temperature. The rate of evolution of water vapour appeared to increase slightly at this temperature. Raising the temperature to 300° C was followed by the evolution of more ammonia from the sample and very small increase in the rate of evolution of water vapour. At 400° C, the rate of evolution of ammonia was less than that at 300° C, because presumably the samples were almost completely decomposed at this temperature. The temperature of 300° C corresponds to the temperature of maximum ammonia evolution during decomposition for the monoclinic and freeze-dried samples of APT. This rate was very nearly equal to the rate of evolution of ammonia at 200 and 300° C for the orthorhombic APT. Raising the temperature to 500° C caused a further decrease in the ammonia content in the gas phase. However, the rate of evolution of water vapour from 300° C onwards remained more or less constant.

The above observations led to the postulation that the thermal decomposition of APT is characterized by a slow rate of evolution of water vapour up to 200° C followed by a steady rate of evolution (which is greater than the rate at 200° C) until complete decomposition of APT occurs at around 500° C. The evolution of ammonia begins at temperatures above 100° C and attains a maximum rate at around 300° C.

3.3. X-ray diffraction analysis

All the decomposition products of the samples of APT were blue in colour and are, therefore, referred to as "blue tungsten oxide". The freeze-dried sample of APT yielded a product of decomposition which gave a characteristic diffraction pattern that was identical to those given by the other two samples. The analysis of the diffraction pattern in Table II indicates that the completely decomposed samples were composed of a mixture of WO_3 and $WO_{2.9}$. The major number of peaks in the diffraction pattern were, however, attributable to WO_3. However, in no case was it possible to obtain pure yellow tungsten trioxide by thermal decomposition of any of the samples of APT in nitrogen. Pure tungsten trioxide could be obtained by heating the blue oxide in air at 500° C for a few minutes.

No diffraction pattern of any form was obtained for the products of partial decomposition produced in the temperature range 100 to 300° C from all the samples of APT. However, all products obtained after partial decomposition at 315° C were found to give X-ray diffraction patterns which corresponded to the mixture of the monoclinic and orthorhombic forms of APT with detectable amounts of tungsten triodixe. On decomposition at subsequent higher temperatures, the amount of tungsten trioxide in the products increased considerably.

The absence of any X-ray diffraction pattern for partial decomposition of the crystalline commercial samples of APT in the temperature range 100 to 300° C may be explained by the formation of amorphous ammonium metatungstates according to the following equations:

$$5(NH_4)_2O.12WO_3.11H_2O$$
$$\rightarrow 3((NH_4)_2O.4WO_3.H_2O) + 4NH_3 + 4H_2O \quad (1)$$

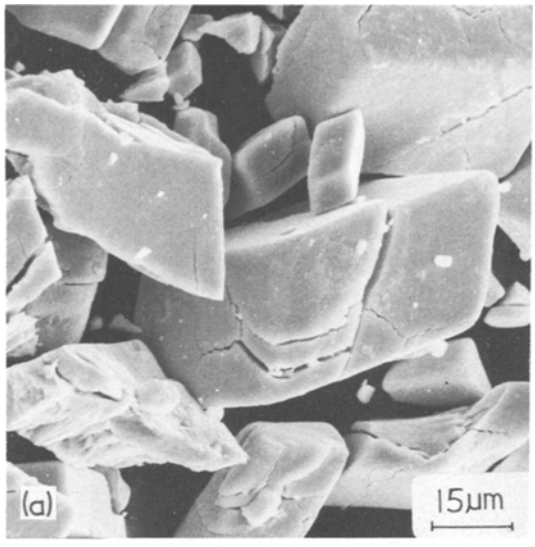

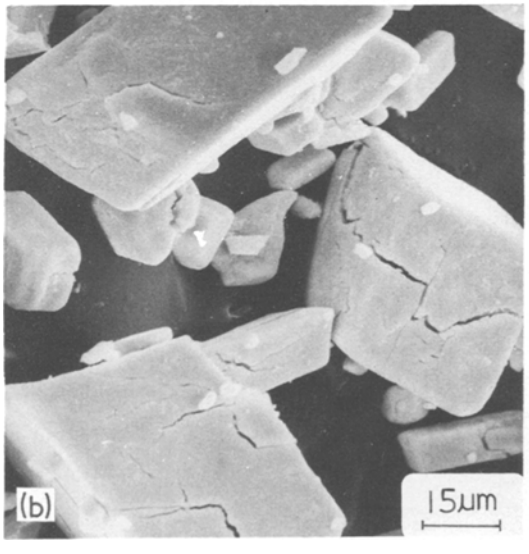

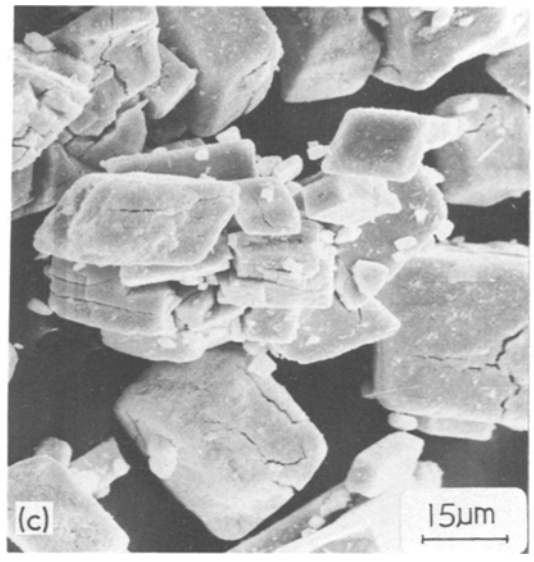

Figure 9 Oxide produced from monoclinic APT. (a) 500° C, (b) 700° C, (c) 900° C.

$$5(NH_4)_2O.12WO_3.5H_2O$$

$$\rightarrow 3((NH_4)_2O.4WO_3.H_2O) + 4NH_3 + 4H_2O \quad (2)$$

This was substantiated by the evolution of ammonia and water vapour at temperatures in excess of 100° C, detected in the study of the evolved gases. This formation of ammonium metatungstate by baking crystalline ammonium paratungstate in the temperature range 150 to 380° C has been reported previously [11, 12] and is confirmed in the present study. The reappearance of detectable amounts of APT in the product after decomposition at 315° C is postulated to be due to the rearrangement of the ammonium metatungstate above 300° C according to the following equations:

$$5((NH_4)_2O.4WO_3.3H_2O)$$

$$\rightarrow 5(NH_4)_2O.12WO_3.11H_2O + 8WO_3 + 4H_2O \quad (3)$$

$$5((NH_4)_2O.4WO_3.H_2O)$$

$$\rightarrow 5(NH_4)_2O.12WO_3.5H_2O + 8WO_3. \quad (4)$$

The driving force for Reactions 3 and 4 is the formation of the new phase, tungsten trioxide, from the ammonium metatungstate. The appearance of tungsten trioxide in the decomposition products of APT was observed only above 300° C when the temperature range of the ammonium metatungstate formation had been exceeded.

Thus, it appears that the thermal decomposition of APT occurs via the formation of ammonium metafungstate at the temperature range of 100 to 300° C, followed by the reappearance of some crystalline APT at 315° C together with some tungsten trioxide. On raising the temperature further, increasing quantities of tungsten trioxide are formed until the samples are fully decomposed. An interesting observation is the fact that the undecahydrate does not decompose to the pentahydrate before producing the blue oxide, as may be expected by comparison with some other hydrated inorganic salts.

3.4. Particle size and morphology

The thermal decomposition products of the orthorhombic APT at 500, 700 and 900° C, as

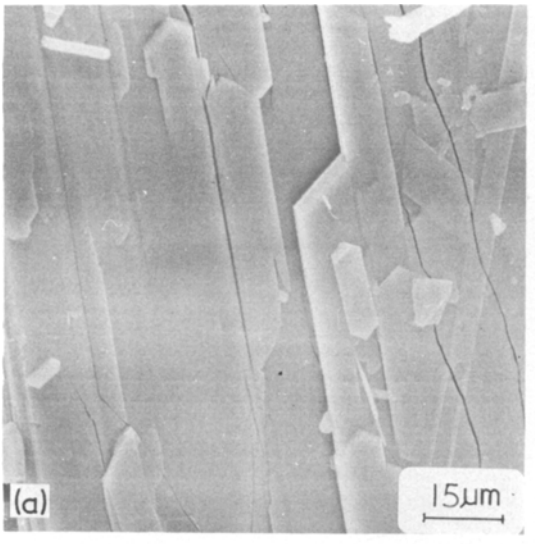

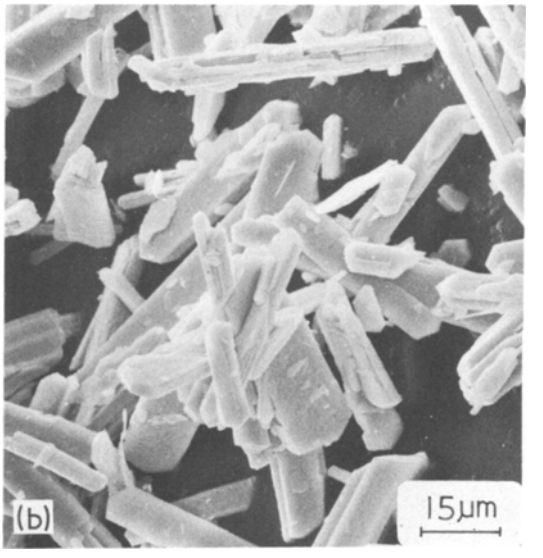

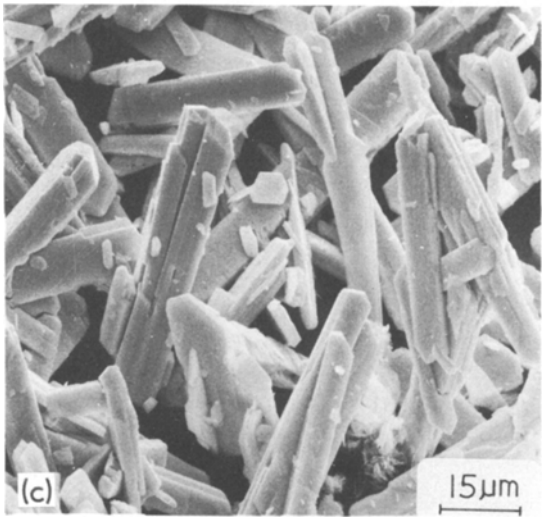

Figure 10 Oxide produced from orthorhombic APT. (a) 500° C, (b) 700° C, (c) 900° C.

shown in Fig. 10a, b and c, were found to be pseudomorphs of the original APT crystals and to retain all the particle characteristics of the starting material. It can be seen that cracks have not been produced in the particles by the elimination of ammonia and water vapour and the consequent contraction in volume of the crystals. Thus, it appears that the lattice strain in the particles caused by the conversion of the orthorhombic APT to orthorhombic tungsten oxides has been accommodated without change in the original particle morphology. Hence, neither excessive reduction of the particle sizes during thermal decomposition at lower temperature, nor appreciable particle growth at higher temperatures has taken place in this sample.

In contrast to the orthorhombic sample, the monoclinic APT gave products of decomposition at 500° C which contained cracks in almost every particle as shown in Fig. 9a. In some cases, the equiaxed monoclinic crystals appeared to have disintegrated into smaller irregular particles by fracture during decomposition. This phenomenon was more pronounced at higher temperatures of 700 and 900° C as shown in Fig. 9b and 9c, respectively. This is shown in the determination of the particle size analysis in Table VI where the weight % of particles in the range 5 to 12 μm has increased at 800° C compared to that at 500° C. The formation of cracks in the particles produced in this sample is associated with the contraction in volume of the crystals and the change in crystal structure from monoclinic to orthorhombic during decomposition. The strain developed in the lattice in this case apparently cannot be accommodated within the particle. After decomposition at 900° C, the particles were clustered together as shown in Fig. 9c where both relatively small and large particles seem to be interlocked, thus forming a large irregular particle. This phenomenon was observed in the particle size analysis in Table VI where the weight % of particles above 38 and 47 μm sizes were apparently increased at higher temperature with respect to those at 500° C.

The typical morphologies of the particles produced by thermal decomposition of the freeze-dried APT at 500, 700 and 900° C are shown in

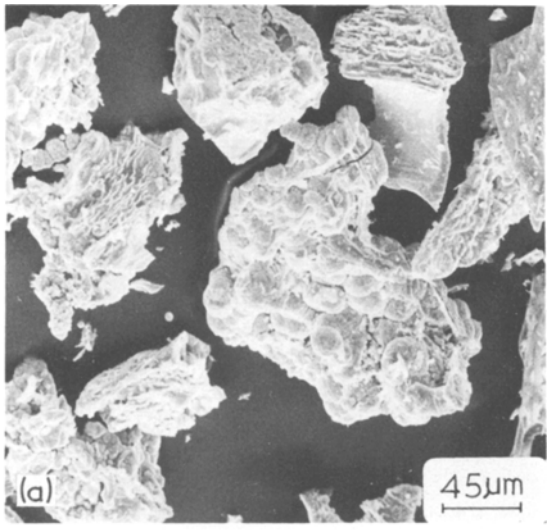

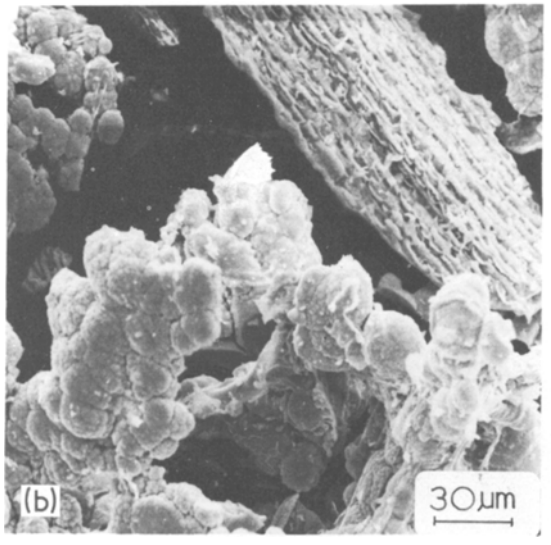

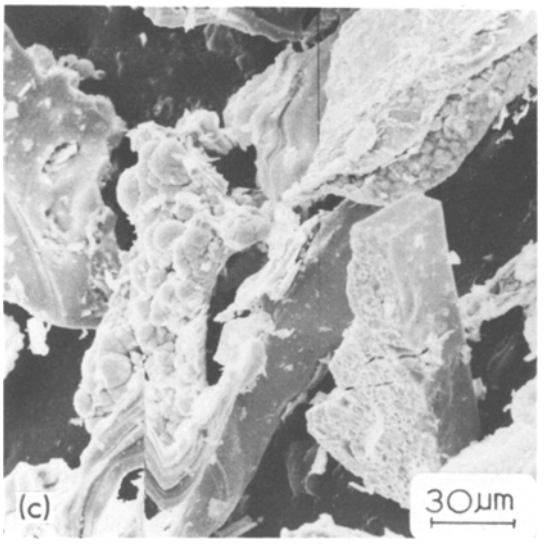

Figure 11 Oxide produced from freeze-dried APT. (a) 500° C, (b) 700° C, (c) 900° C.

Fig. 11a, b and c, respectively, and can be seen to be pseudomorphs of the original material. The oxide particles can be seen to possess the open structure and multiparticulate nature of the freeze-dried APT even after the highest temperature of decomposition of 900° C. No cracks were observed in the products produced by thermal decomposition at lower or higher temperature and this must be explained by similar reasons to those suggested for the orthorhombic APT. No additional clustering of the particles in this sample appeared to have taken place after decomposition at higher temperatures of 700 or 900° C.

4. Conclusions

(1) The three samples of APT, the monoclinic $5(NH_4)_2O.12WO_3.5H_2O$, the orthorhombic $5(NH_4)_2O.12WO_3.11H_2O$ and the freeze-dried APT decomposed in nitrogen above 450° C to form blue tungsten oxide which consists of a mixture of WO_3 and $WO_{2.9}$. The kinetics of decomposition of all the samples of APT have been found to be similar.

(2) The particle morphologies of the decomposition products of the orthorhombic and freeze-dried APT samples have been found to be pseudomorphs of the parent materials. The monoclinic APT after decomposition yields oxide which possesses a large number of cracks and indicates an appreciable degree of mechanical breakdown of the original particles.

(3) After partial decomposition of APT in the temperature range 100 to 300° C, no diffraction pattern of any form is obtained from the products. This suggests the formation of amorphous ammonium metatungstate. Decomposition above 315° C causes the appearance of tungsten trioxide in the product.

Acknowledgements

The authors would like to thank Professor E. Smith for the provision of general laboratory facilities, the University of Manchester for the award of the Bedson fellowship for one year to one of the authors (AKB), and the Institution of Mining and Metallurgy for the award of the Stanly Elmore postdoctorial research fellowship to the same

author (AKB) to allow postdoctorial work to be continued in this general subject area.

References

1. R. L. RIPLEY and H. LAMPREY, in "Ultrafine Particles", edited by W. E. Kuhn (Wiley, New York, 1963) p. 262.
2. L. RAMQVIST, in "Modern Developments in Powder Metallurgy", Vol. 4, edited by H. H. Hausner (Plenum Press, New York, 1971) p. 75.
3. J. H. OXLEY, E. A. BEIDLER, J. M. BLOCHER, C. J. LYONS, R. S. PARK and J. H. PEARSON, *Nucl. Appl.* 1 (1965) 567.
4. J. M. GOMES, K. UCHIDA and M. M. WONG, U.S. Bur. Mines, Rept. Invt. 7344 (1970) p. 8; 7580 (1971) p. 10.
5. A. B. SUCHKOV, G. V. RUMYANTSEVA, A. R. DEMACHEV and N. V. ZHUKOVA, *Sov. Powder Met. and Met. Cer.* 12 (1971) 941.
6. T. KH. IMANOV, R. N. BAZAROV and A. L. KAL'KOV, *Electrokhimiya* 10 (1974) 1223.
7. A. LANDSBERG and T. T. CAMPBELL, *J. Metals* 17 (1965) 856.
8. F. K. ROEHRIG and T. R. WRIGHT, *J. Vac. Sci. Tech.* 9 (1972) 1368.
9. S. H. GELLES and R. K. ROEHRIG, *J. Metals* 24 (1972) 23.
10. A. K. BASU and F. R. SALE, *J. Mater. Sci.* 10 (1975) 571.
11. V. CHIOLA, J. M. LAFERTY and C. D. VANDERPOOL, U.S. Patent No. 3, 175, 881, 30 March (1965).
12. K. C. LI and C. Y. WANG, "Tungsten – Its History, Geology, Ore Dressing, Metallurgy, Chemistry, Analysis, Application and Economics" (Reinhold, New York, and Chapman and Hall, London, 1955).

Received 18 October and accepted 28 October 1976.